Biosensors and Bioelectronics
June 2007, Volume 22, Issue 12, Pages 2884-2890
http://dx.doi.org/10.1016/j.bios.2006.12.009

Anti-rabbit immunoglobulin G detection in complex medium by PM-RAIRS and QCM Influence of the antibody immobilisation method

Elisabeth Briand[a], Michèle Salmain[b], Chantal Compère[c] and Claire-Marie Pradier[a, *]

[a]Laboratoire de Réactivité de Surface, UMR CNRS 7609, Université Pierre et Marie Curie, 4 place Jussieu, 75252 Paris Cedex 05, France
[b]Laboratoire de Chimie et Biochimie des Complexes Moléculaires, UMR 7576, Ecole Nationale Supérieure de Chimie Paris, 75231 Paris Cedex 05, France
[c]Département Essais et Recherches Technologiques, Interfaces et capteurs, IFREMER, Centre de Brest, BP 70, 29280 Plouzané, France

*: Corresponding author : Claire-Marie Pradier, email address : pradier@ccr.jussieu.fr

Abstract:

Two antibody immobilisation procedures were compared to set up an immunosensor for goat anti-rabbit immunoglobulin (anti-rIgG), i.e. rIgG covalently bound or immobilised via affinity to protein A (PrA). In both cases, the first layer of protein was covalently bound to a mixed self-assembled monolayer (SAM) of mercaptoundecanoic acid (MUA) and mercaptohexanol (C6OH) on a gold surface. The elaboration of the sensitive surfaces, as well as their selectivity and sensitivity were studied step by step by polarization modulation-reflection absorption infra-red spectroscopy (PM-RAIRS) and quartz crystal microbalance (QCM) with impedance measurement. QCM measurements showed that the viscoelastic properties of the antibody layer were markedly modified during the antigen recognition when the antibody was bound by affinity to PrA. The specific detection of antigen within a complex medium was assessed by PM-RAIRS thanks to the grafting of cobalt-carbonyl probes. Affinity constants between the immobilised rIgG and the anti-rIgG were determined from PM-RAIRS analysis.

Keywords: Immunosensors; QCM; PM-RAIRS; rIgG immobilisation

1. Introduction

Biosensors provide a rapid, convenient and low cost alternative to conventional analytical methods, like HPLC or ELISA, for detecting, and in some cases for assaying, an analyte in a complex medium. An immunosensor relies on the ability of an immobilized antibody to recognize its associated antigen in a very complex medium. The strategy chosen to create the sensing layer should enable to control both the amount and the orientation of the antibody on the transducer while preserving its bioactivity.

Immobilisation of biomolecules on gold surfaces is readily achieved by making use of Self-Assembled Monolayers (SAMs) (Wink et al. 1997). Alkylthiols spontaneously chemisorb from solution onto gold surfaces and form stable, densely packed, crystalline-like thiolate films in a very reproducible manner (Bain et al. 1989, Laibinis et al. 1991, Nuzzo et al. 1990, Porter et al. 1987b, Whitesides and Laibinis 1990). Mixed SAMs are generally constituted of one thiolate with a functional headgroup (like a carboxylic acid) at low mole fraction and of another "diluting" thiolate at high mole fraction to minimize steric hindrance, denaturation of the protein (Guiomar et al. 1999) as well as non specific interactions (Frederix et al. 2003, Ge and Lisdat 2002).

Among the various published strategies to immobilize antibodies on a solid surface, i.e. direct physisorption (Bizet et al. 1998, Caruso et al. 1996, Chang et al. 1995, Ouerghi et al. 2002), covalent binding (Babacan et al. 2000, Caruso et al. 1996, Cui et al. 2003b, Disley et al. 1998, Eun et al. 2002, Frederix et al. 2004, Grubor et al. 2004, Pei et al. 2001, Su et al. 1999, Susmel et al. 2003), or affinity binding via the biotin / avidin couple (Boozer et al. 2003, Cui et al. 2003a, Ouerghi et al. 2002) or via *Staphylococcus aureus* Protein A (PrA), two of them were chosen in the present work and compared. Several examples of immunosensing devices based on the immobilization of specific antibodies *via* a layer of PrA have been reported (Atashbar et al. 2005, Babacan et al. 2000, Galli Marxer et al. 2003, Grubor et al. 2004, Kaur et al. 2004, Lin and Tsai 2003, Lu et al. 2000, Michalzik et al. 2005a, Muramatsu et al. 1987, Saha et al. 2003); the benefit is a proper orientation of the antibody (Lu et al. 1996) and an easy immunosensor regeneration (Quinn et al. 1999).

In this work, a mixed SAM of MUA and C6OH, at a 1:3 mole ratio in solution, was assembled on gold surfaces. Two antibody binding methods were tested: i) covalent binding to the carboxylic acid moieties of the mixed SAM or, ii) affinity binding via Protein A covalently linked to the acid moieties (Scheme in supplemental information). Each binding step was characterised by PM-RAIRS and QCM. While PM-RAIRS has been extensively

used to characterise adsorbed molecular layers, QCM has become, since 1972 (Shons et al. 1972), one of the most useful techniques to monitor immunosensing processes and more generally to detect targets like proteins (Bizet et al. 1998, Caruso et al. 1996, Kösslinger et al. 1995, Liu et al. 2001, Michalzik et al. 2005a, Michalzik et al. 2005b, Muramatsu et al. 1987, Shen et al. 2005, Su et al. 1999), viruses (Eun et al. 2002), cells (Kim and Park 2003, Olsen et al. 2003, Su and Li 2004, Su and Li 2005) and toxins (Lin and Tsai 2003, Pribyl et al. 2003, Tang et al. 2002).

Binding of proteins to surfaces induces frequency shifts due to the molecules themselves but also to water hydrodynamically coupled to them; moreover, modifications in the viscoelastic properties of the adlayers may involve deviation of the frequency shift from the linear dependence on mass deposition predicted by Sauerbrey (Fredriksson et al. 1998, Galli Marxer et al. 2003, Gry Hemmersam et al. 2005, Höök et al. 2001, Höök et al. 2002, Lord et al. 2006, Olsen et al. 2003, Voivona et al. 2002). If the added overlayer slips at the interface with the quartz crystal, or if it is "soft" enough to be reversibly strained by the shear motion, it indeed induces viscosity changes detectable via the measurement of dissipation (Höök et al. 1998, Rodahl et al. 1996).

Reflection-absorption IR spectroscopy (RAIRS) is a vibrational technique sensitive to molecules bound at the surface of a highly reflective metallic substrate. Modulation of the polarization (PM) avoids the recording of a background spectrum and eliminates the contribution of the isotropic environment. IR spectroscopy has been widely used to study SAMs on metallic surfaces as well as peptide or protein grafting (Lieberg et al. 1985, Pradier et al. 2002).

These two techniques are complementary: PM-RAIRS provides information on the chemical nature of the adsorbed molecules and the chemical bonds formed at each step. QCM measurements yield mass uptakes and layer viscoelastic properties (Hemmersam et al. 2005, Lucklum and Hauptmann 2000a, Lucklum and Hauptmann 2000b).

2. Material and methods

2.1. Chemicals

1-mercapto-11-undecanoic acid (MUA), 1-mercapto-6-hexanol (C6OH), *N*-hydroxysuccinimide (NHS), N-(3-dimethylaminopropyl)-N'-ethylcarbodiimide hydrochloride (EDC) were purchased from Aldrich (France). Rabbit IgG (rIgG), goat serum and bovine serum albumin (BSA) were purchased from Sigma (France), recombinant Protein A (PrA)

from Pierce (Perbio, France). Buffers were prepared with MilliQ grade water and all solvents were reagent-grade. Reagents were used without any further purification. Experiments were carried out at room temperature.

Labelling of anti-rIgG molecules with $Co_2(CO)_6$ probes was performed following a procedure previously described (reff). The concentration of $Co_2(CO)_6$ entities $n_{Co2(CO)6}$ determined by UV-Vis spectroscopy, combined to the protein concentration $n_{Anti\text{-}rIgG}$ determined by the Bradford's assay gave a ratio $n_{Co2(CO)6} / n_{Anti\text{-}rIgG}$ of 22:1 (data not shown).

2.2. Instrumentation:

2.2.1. PM-RAIRS measurements

Glass substrates (11 x 11 mm), successively coated with a 50 Å layer of chromium and a 200 Å layer of gold, were purchased from Arrandee (Werther, Germany). The gold-coated substrates were annealed in a flame to ensure a good crystallinity of the topmost layers. The FTIR instrument is a commercial NICOLET Nexus spectrometer. The external beam was focused on the sample, at an optimal incident angle of 75°. A ZnSe grid polarizer and a ZnSe photoelastic modulator, modulating the incident beam between p and s polarizations (HINDS Instruments, PEM 90, 37 kHz), were placed prior to the sample. The light reflected at the sample was focussed on a nitrogen-cooled MCT detector. The sum and difference interferograms were processed and Fourier-transformed to yield the differential reflectivity $\Delta R/R=(Rp-Rs)/(Rp+Rs)$ which is the PM-IRRAS signal. 128 scans were recorded at 8 cm^{-1} resolution for each spectrum.

2.2.2. QCM measurements

AT-cut planar quartz crystals, 14 mm diameter, with a 5 MHz nominal resonance frequency (QuartzPro, Sweden) were used. Two gold electrodes were evaporated on both sides of crystals. Their diameters are 10 mm for the upper one and 5 nm for the bottom one in order to avoid liquid electrical contribution on the resonant frequency (Rodahl et al. 1996). Only one face of the quartz crystal was in contact with the solutions. The frequency and dissipation variations at the 3^{rd}, 5^{th}, 7^{th}, 9^{th} overtones were monitored using a QCM-Z500 apparatus (KSV, Finland). This QCM set up allows the simultaneous recording of resonance frequency and impedance between the two electrodes. Dissipation data were automatically calculated by an internal software. To improve the stability, the QCM cell (2mL) was

temperature-controlled at 25°C thanks to a Peltier element. Mass changes on the surface of a piezoelectric crystal induce variations in the resonance frequency according to

$$\Delta f = -2\Delta m \times n f_0^{\,2} \Big/ A(\mu_q \rho_q)^{1/2},$$

where n is the overtone number, μ_q is the shear modulus of the quartz ($2.947.10^{11}$ g/cm.s²), ρ_q is the density of the quartz (2.648 g/cm^3) and $\Delta m/A$ is the surface density (Sauerbrey 1959). This equation assumes that the added mass is strongly coupled to the resonator.

2.3. Elaboration of the sensors

2.3.1. Formation of the mixed SAM

The gold-coated glass substrates and quartz crystals were rinsed in absolute ethanol during 15 min and dried under nitrogen before adsorption. The substrates were immersed in a freshly prepared binary mixture of thiols in absolute ethanol at a total concentration of 10 mM for 3 h (Hobara et al. 1999) to ensure an optimal homogeneity of the mixed layer. The substrates were rinsed in ethanol and dried under nitrogen.

2.3.2. Immobilization of PrA

The substrates were treated with an aqueous solution of NHS (20 mM) and EDC (10 mM) for 2 h, and immersed in a solution of PrA (10 mg/L) in 10 mM PBS pH 7.4 for 2 h. The residual NHS esters were blocked by treatment with 1 M ethanolamine pH 9.0 for 20 min. Finally, the substrates were immersed in a 100 mg/L solution of BSA in 10 mM PBS pH 7.4 for 2 h. Before each new treatment, the substrates were extensively rinsed in pure water and dried.

2.3.3. Binding of rabbit IgG

Covalent binding of rabbit IgG was achieved by immersion of the SAM functionalized gold surfaces in rIgG solutions (0.1 g/L in PBS buffer) for 2 h. Alternatively, rabbit IgG was bound by affinity on immobilized PrA by immersion of PrA-coated substrates in the same rIgG solution for 2 h. The substrates were then rinsed extensively with water and dried before PM-RAIRS analysis. All QCM measurements were performed after SAM formation and activation by NHS-EDC. The protein (rIgG, or PrA + rIgG) binding steps were monitored by QCM in-situ in PBS. Reactions were considered as complete when equilibrium was reached. The rinsing steps were done with PBS without any drying procedures.

2.4. Tests of specificity by PM-RAIRS

Solutions of anti-rIgG, labelled with $Co_2(CO)_6$ probes of concentrations ranging from 0 to 75 mg/L were prepared in PBS containing 0.15% v/v goat serum (albumin and immunoglobulin). The various solutions were successively spotted onto the functionalized surfaces. After 45 min incubation, the substrates were extensively washed with water, dried and analysed by PM-RAIRS.

2.5. Tests of specificity by QCM

Diluted goat serum (0.15% v/v in PBS) was introduced into the cell. Once the equilibrium was reached, a solution containing diluted goat serum (0.15% v/v in PBS) and anti-rIgG (20 mg/L) was allowed to react with the functionalized quartz crystal. The samples were rinsed by three successive injections of PBS.

3. Results and discussion

3.1. Elaboration of the sensitive surfaces

3.1.1. Formation of the mixed SAM

The choice of the mole fraction of MUA was made after a systematic characterisation of mixed SAMs resulting from immersions of gold-coated substrates in MUA/C6OH solutions at various concentrations. An MUA mole ratio of 0.25 appeared to yield the optimal activation rate of the terminal acid functions (Briand et al.). The formation of a mixed SAM, was checked thanks to the presence of various bands characteristic of OH or COOH moieties. Moreover, the C-H stretching vibration modes of the SAM alkyl chains, very sensitive to the packing density (Laibinis et al. 1992, Nuzzo et al. 1990, Porter et al. 1987a), indicated that, the mixed SAM was poorly ordered (see supporting information, ν_{asCH} band at 2928 cm^{-1}). This is not surprising for mixed SAM's of thiols with different alkyl chain lengths (Frederix et al. 2004, Laibinis et al. 1992). XPS analysis of one SAM-coated sample indicated a surface concentration close to that in solution (data not shown).

3.1.2. Covalent binding of rIgG

3.1.2.1.Immobilisation of rIgG.

The gold surface was analysed by PM-RAIRS after activation of the carboxylic acid SAM with the mixture of NHS and EDC, then after treatment with the solution of rIgG. Covalent binding of rIgG on the surfaces was assessed by the appearance of typical amide I and II bands at 1660 and 1550 cm^{-1} and the simultaneous decrease of the ester $\nu_{C=O}$ bands at 1815, 1785 and 1743 cm^{-1} (see supplemental information). These bands completely disappeared after reaction in ethanolamine solution. The total peptide band area (1550 + 1660 cm^{-1}) was equal to 10.7 a.u..

In situ QCM measurements performed during exposure to rIgG solution (Fig. 2a) showed an immediate significant frequency shift. Neither a large dissipation nor differences between the normalized frequency shifts at the various harmonics were observed. The $\Delta D/\Delta F$ value at equilibrium at the third harmonic was equal to 0.01. We assumed that no dissipative mechanisms occurred during the adsorption process and that the Sauerbrey equation was thus valid. The normalised frequency shift, 58 Hz, yielded a surface density of 1010 ng/cm². Considering a rabbit IgG molecule as a sphere of 10 nm diameter (Nellen et al. 1988), a complete monolayer should yield a surface coverage close to 300 ng/cm² (Frederix et al. 2004). The coverage calculated from these experiments corresponds to ca 3 monolayers, explained by the mass of hydrodynamically coupled water (Caruso et al. 1997, Höök et al. 2002), not distinguishable from protein by QCM, and possibly representing up to 400% of the mass uptake measured by QCM in solution (Caruso et al. 1997, Höök et al. 2001, Höök et al. 2002).

All PM-IRAIRS and QCM data acquired along the elaboration and tests of the sensing surfaces are summarised in Fig. 1.

3.1.2.2. Blocking step by BSA.

After the rIgG binding step, a solution of BSA was introduced and the BSA uptake was evaluated from QCM (in situ) and PM-RAIRS (ex situ). The increase of the IR amide band areas was less than 1% and the QCM frequency shift corresponded to a mass uptake of 3%. This confirmed the formation of a complete rIgG monolayer by covalent binding to the SAM.

3.1.3. Immobilisation of rIgG by affinity via PrA.

3.1.3.1. Grafting of PrA

From PM-RAIRS data, chemisorption of PrA to the SAM-coated gold surfaces induced the same chemical changes as the covalent binding of rIgG, i.e. a decrease of the $\nu_{C=O}$ bands characteristic of the activated acid moieties and the appearance of the amide I and amide II bands (spectra not shown). The total peptide band area corresponded to 2.4 a.u..

The binding of PrA to the mixed SAM was also monitored by QCM. The frequency shifts at the different overtones, normalized as $\Delta F_n/n$ (with n=3, 5, 7, 9) showed no great differences, all roughly equal to 23 Hz; only the results obtained at the third overtone will thus be reported. Once again, the dissipation shift being equal to 2.10^{-6}, the Sauerbrey equation could be applied (Gry Hemmersam et al. 2005). The so calculated total adsorbed mass yielded a surface density of 380 ng/cm². The PrA size, being around 3 nm diameter (Brookhaven Data Bank), this value leads to a sub-monolayer coverage.

3.1.3.2. Blocking step with BSA.

BSA is an efficient blocking agent and does not bind to protein A (Galli Marxer et al. 2003). After covalent grafting of PrA, treatment of the surface with the solution of BSA led to an increase (+30%) of the PM-RAIRS amide I + amide II band area (see Fig.1). This confirms that the surface was not saturated after PrA grafting.

The QCM normalized frequency shifts, corresponding to the binding of BSA after PrA grafting was 6 Hz (Fig. 1 and 2b) corresponding to a mass uptake of 90 ng/cm². Having in mind that one monolayer of BSA would yield 200 to 600 ng/cm² depending on the orientation of the molecules, this indicates that a significant amount of BSA was adsorbed in addition to grafted PrA (25% added mass). RAIRS and QCM measurements are in excellent agreement.

3.1.3.3. Rabbit IgG binding to PrA

The increase of the $\nu_{C=O} + \delta_{N-H}$ band area, after immobilisation of rIgG, reported in Fig. 1 (PM-RAIRS analysis), was equal to 5 a.u., corresponding to 0.5 rIgG per PrA. This ratio is in good agreement with previously published results, 0.2 to 0.6 IgG per PrA (Atashbar et al. 2005, Michalzik et al. 2005b, Muramatsu et al. 1987, Pribyl et al. 2003). The amount of rIgG bound by affinity to PrA was twice lower than the amount of rIgG covalently bound to the mixed SAM.

QCM results showed a frequency shift indicating the binding of rIgG with a weak energy dissipation (Fig. 1 and 2b). The corresponding mass increase was 715 ng/cm², i.e. a ratio of 0.5 rIgG per PrA, in agreement with the IR data. The $\Delta D/\Delta F$ (10^{-6} Hz^{-1}) ratio, measured at the third overtone after the equilibrium was reached, was equal to -0.04, while it

was equal to -0.01 in the case of rIgG covalently bound to the SAM. This suggests that the dissipation per mass unit of the whole adlayer was larger when rIgG was immobilised by affinity via PrA. The adlayer formed in this case was likely more flexible than in the former case where multiple bondings via lysine residues increase the rigidity of the layer.

3.2. Tests of specificity

To determine the extent of non specific binding, the two sensing surfaces were allowed to react with diluted goat serum (0.15 % v/v) in PBS. PM-RAIRS results indicated a slight increase of the amide bands, lower than 10% on the IgG bound via PrA layer ($rIgG_{PrA}$), and even weaker on the surface modified by covalently bound rIgG ($rIgG_{cov}$).

The frequency shifts recorded by QCM confirmed the binding of molecules from the goat serum (Fig. 2a, b). Compared to the binding of rIgG, the corresponding mass increase was almost zero on the $rIgG_{PrA}$ surface and 10% on the $rIgG_{cov}$ surface. The non specific adsorption of proteins was weak whatever the mode of attachment of the antibodies.

3.3. Anti-rIgG recognition by QCM.

The efficiency of the two sensing layers was evaluated by assaying the specific recognition of anti-rIgG diluted in the goat serum solution (Fig. 2a, b). The concentration of specific antigen was 20 mg/L, in a solution containing c.a. 100 mg/L of goat serum proteins. Huge frequency shifts were observed for both surfaces, suggesting an efficient and specific recognition of anti-rIgG. This led to apparent antigen to antibody ratios of 1.4 for the $rIgG_{cov}$ surface and 2.9 for the $rIgG_{PrA}$ surface.

Fig. 3 shows the dissipation changes as a function of Δf during the binding of anti-rIgG to the $rIgG_{Cov}$ and $rIgG_{PrA}$ surfaces and significant differences are worth noticing. On the $rIgG_{cov}$ surface, the dissipation increased when the anti-rIgG solution came in contact with the sensor surface, then, it remained constant; the slope, close to zero ($< 10^{-3}$), compared to the $\Delta D/\Delta f$ value of -0.01 upon rIgG covalent binding, can be interpreted as a stiffering of the whole protein layer (Hemmersam et al. 2005). Moreover, the normalized frequency shift did not show any dependence with the considered overtone as already observed for a similar system by Bizet et al. (Bizet et al. 1998). Conversely, on the $rIgG_{PrA}$ surface, the normalized frequency shift decreased when the harmonic number increased and the dissipation increased

linearly with the frequency shift, with a $\Delta D/\Delta f$ slope equal to -0.01; the $\Delta D/\Delta f$ was equal to -0.04 upon rIgG binding on PrA, thus, the viscoelastic properties of the protein layer was less modified in the latter case. Moreover, the number of bound antigens was higher which, in some way contributes to the $\Delta D/\Delta f$ decrease; in other words, at equal number of bound molecules the recognition of antigens is expected to significantly modify the layer on IgG_{cov} but not on $rIgG_{PrA}$; this is most likely due to different orientations and/or accessibilities of the antibodies on the two layers.

Clearly, at that step, the QCM does not work in a pure gravimetric regime; it provides valuable structural information which implies that the layers of rIgG's, covalently or by affinity attached, display different affinities for the antigens, in relation to their rigidities (Lucklum and Hauptmann 2000b).

3.4. Anti-rIgG recognition by PM-RAIRS.

The use of $Co_2(CO)_6$ labelled anti-rIgG allowed us to assess the specific binding of the targeted antigens in a complex medium (the same diluted goat serum as above).

Both sensing surfaces were treated with solutions of labelled antigens at increasing concentrations (see PM-RAIRS spectra for the $rIgG_{PrA}$ surface in Fig. 4). The amide I and amide II bands increased with the anti-rIgG concentration. So did the characteristic $\nu_{MC\equiv O}$ bands of the cobalt-carbonyl probe at 2094, 2052 and 2025 cm^{-1}. The amide I and II band area increased linearly with the 3 $\nu_{MC\equiv O}$ signals (see insert of Fig. 4), confirming that only specific interactions occurred. The IgG_{cov} sensing surface behaved similarly.

The amide I and II bands area was then plotted as a function of the antigen concentration (Fig. 5). The affinity constants K of the immobilized antibody for anti-rIgG were calculated assuming a Langmuir-type adsorption model (Liu et al. 2001, Sakai et al. 1999, Soh et al. 2003). Experimental data were fitted with the non linear curve fitting procedure of the Origin software (Microcal, Northampton, MA) according to the following expression:

$$A = A_{\max} \times K \times C \,/\, 1 + K \times C$$

where A represents the sum amide I + amide II areas, K, the affinity constant and C, the antigen concentration (mg/L). Very good correlations between fitted curves and experimental

data points (Fig. 5a and b) were obtained with R^2 greater than 0.99 for both surfaces. The calculated number of binding sites A_{max} was equal to 14.4 ± 0.6, and 17.1 ± 0.5 for $rIgG_{PrA}$ and $rIgG_{Cov}$, respectively. A_{max} was only slightly higher for the $rIgG_{cov}$ surface although twice more antibody molecules were immobilised on this surface. The amount of bound antigens per antibody was, at a maximum, equal to 2.7 on the $rIgG_{PrA}$ surface and 1.5 on the $rIgG_{Cov}$ surface. These high ratios (> 1) may be explained by the polyclonal nature of goat anti-rIgG that is directed against the whole rIgG molecule. The latter is likely to bear several epitopes, each of them possibly binding one anti-rIgG. The higher ratio measured for the $rIgG_{PrA}$ surface may result from the higher number of accessible epitopes because of the lower surface density of rIgGs.

The calculated affinity constants K were $2.3.10^7$ and $8.7.10^6$ M^{-1} for the $rIgG_{PrA}$ and $rIgG_{Cov}$ surfaces, respectively, in good agreement with previously published results for various antigen/antibody couples (Lu et al. 2000, Pribyl et al. 2003, Sakai et al. 1999, Soh et al. 2003). It may appear surprising that the binding constants of the rIgG / anti-rIgG couple depended on the rIgG immobilisation method, but as the goat anti-rIgG is a polyclonal antibody these K values represent an average of the individual affinity constants between the various epitopes and paratopes which may differ according to the immobilisation method.

If one assumes a standard deviation on the A determination of 0.1, the limit of detection (l.o.d.) can be calculated from the following equation (Frederix et al. 2003):

$$\text{l.o.d.} = {}^{0.3}\!\!\diagup\!\!_{K \times (A_{max} - 0.3)},$$

leading to 0.14 mg/L and 0.31 mg/L for the $rIgG_{PrA}$ and $rIgG_{Cov}$ surfaces, respectively. Note that the lowest l.o.d. was obtained for the $rIgG_{PrA}$ surface, when the amount of immobilized antibody was the lowest. Babacan et al. compared the limits of detection of *Salmonella* sp by QCM using two similar sensing platforms (physisorbed PrA and covalently bound IgG to a SAM) (Babacan et al. 2000). They found similar l.o.ds for both sensing layers but the results obtained with physisorbed Protein A were more stable and reproducible. Note that protein A studied in Babacan's work was simply physisorbed on the gold surfaces and this is expected to decrease the efficiency of the system as compared to a covalent linkage of PrA (Michalzik et al. 2005b). The l.o.ds determined in this study were acceptable for non amplified systems, even slightly better than previously reported data using other label-free transduction techniques: 10 mg/L of anti-human serum albumin determined by QCM (Liu et al. 2001), 6 mg/L of human IgG by SPR (Disley et al. 1998). Let us recall that the objective of this paper was rather to demonstrate the complementarity of the two techniques, IR and QCM to

characterise biomolecular recognition phenomena than to reach the highest possible sensitivity.

4. Summary and Conclusion

Model immunosensors of goat anti-rIgG were elaborated by covalent grafting of rIgG to a mixed self-assembled monolayer or by binding by affinity to protein A. QCM and PM-RAIRS characterisation techniques were used at each step of the immunosensor elaboration and also for testing the sensitivity and specificity of anti-rIgG binding. The main outputs of this work can be summarised as follows:

- the first layer of proteins on the mixed SAM behaves as a rigid, evenly distributed, protein layer from QCM data at several overtones; water coupled to the protein layer adds to the total mass uptake and makes it difficult to determine the real surface coverage.
- The amount of antibodies immobilised by affinity to PrA and determined by PM-RAIRS was twice lower than when covalently bound to the mixed SAM. This ratio appeared smaller from QCM, probably due to various amounts of coupled water.
- Very weak non specific binding of goat serum proteins were observed on both sensing layers.
- The specific binding of antigens was assessed by labelling with a metallocarbonyl probe.
- Affinity constants were calculated from PM-RAIRS measurements.
- Reasonably good limits of detections were attained by PM-RAIRS measurements without the use of any probe or signal amplification.

In-situ or ex-situ analyses gave different and complementary results. QCM signals obviously included mass uptake due to water; moreover, significant modifications of viscoelastic properties of the layers during the binding process were evidenced. For the first time to our knowledge, PM-RAIRS was used for the detection of labelled antigen in a complex medium as well as for the calculation of binding affinity constants.

Acknowledgement

The Centre National de la Recherche Scientifique, the French Ministry of Research and IFREMER are gratefully acknowledged for financial support.

Supporting information available

Schematic representation of the sensor surfaces. a) rIgG covalently bound to the mixed SAM of MUA and C6OH and b) rIgG immobilized by affinity to PrA covalently bound to the same mixed SAM.

PM-IRRAS spectra of the mixed MUA / C6OH SAM at 1 / 3 mole ratio and after (a) activation by NHS and EDC, (b) chemical binding of rIgG (c) deactivation of the NHS ester functions by ethanolamine are given.

References

Atashbar, M. Z., B. Bejcek, A. Vijh, and S. Singamaneni. 2005. Sens. Actuators B 107: 945-951.

Babacan, S., P. Pivarnik, S. Letcher, and A. G. Rand. 2000. Biosens. Bioelectron. 15: 615-621.

Bain, C. D., E. B. Troughton, Y.-T. Tao, J. Evall, G. M. Whitesides, and R. G. Nuzzo. 1989. J. Am. Chem. Soc. 111: 321-335.

Bizet, K., C. Gabrielli, H. Perrot, and J. Therasse. 1998. Biosens. Bioelectron. 13: 259-269.

Boozer, C., Q. Yu, S. Chen, C.-Y. Lee, J. Homola, S. S. Yee, and S. Jiang. 2003. Sensors Actuators B 90: 22-30.

Briand, E., M. Salmain, C. Compère, and C. M. Pradier. To be published.

Caruso, F., D. Neil Furlong, and P. Kingshott. 1997. J. Colloid Interface Sci. 186: 129-140.

Caruso, F., E. Rodda, and F. N. 1996. J.Colloid Interface Sci. 178: 104-115.

Chang, I.-N., J.-N. Lin, J. D. Andrade, and J. N. Herron. 1995. J. Colloid Interface Sci. 174: 10-23.

Cui, X., R. Pei, Z. Wang, F. Yang, Y. Ma, S. Dong, and X. Yang. 2003a. Biosens. Bioelectron. 18: 59-67.

Cui, X., F. Yang, Y. Sha, and X. Yang. 2003b. Talanta 60: 53-61.

Disley, M., D. C. Cullen, H.-X. You, and C. R. Lowe. 1998. Biosens. Bioelectron. 13: 1213-1225.

Eun, A. J.-C., L. Huang, F.-T. Chew, S. F.-Y. Li, and S.-M. Wong. 2002. J. Virological Methods 99: 71-79.

Frederix, F., K. Bonroy, W. Laureyn, G. Reekmans, A. Campitelli, W. Dehaen, and G. Maes. 2003. Langmuir 19: 4351-4357.

Frederix, F., K. Bonroy, G. Reekmans, W. Laureyn, A. Campitelli, M. A. Abramov, W. Dehaen, and G. Maes. 2004. J. Biochem. Biophys. Methods. 58: 67-74.

Fredriksson, C., S. Kihlman, M. Rodahl, and B. Kasemo. 1998. Langmuir 14: 248-251.

Galli Marxer, C., M. Collaud Coen, and L. Schlapbach. 2003. J. Colloid Interface Sci. 261: 291-298.

Ge, B., and F. Lisdat. 2002. Anal. Chim. Acta 454: 53-64.

Grubor, N. M., R. Shinar, R. Jankowiak, M. D. Porter, and G. J. Small. 2004. Biosens. Bioelectron. 19: 547-556.

Gry Hemmersam, A., M. Foss, J. Chevallier, and F. Besenbacher. 2005. Colloids and Surf. B 43: 208-215.

Guiomar, A. J., J. T. Guthrie, and S. D. Evans. 1999. Langmuir 15: 1198-1207.

Hemmersam, A. G., M. Foss, J. Chevallier, and F. Besenbacher. 2005. Colloids Surf. B: Biointerfaces 43: 208-215.
Hjelm, H., J. Sjodahl, and J. Sjoquist. 1975. Eur. J. Biochem. 52: 395-403.
Hobara, D., T. Sasaki, S.-i. Imabayashi, and T. Kakiuchi. 1999. Langmuir 15: 5073-5078.
Höök, F., B. Kasemo, T. Nylander, C. Fant, K. Sott, and H. Elwing. 2001. Anal. Chem. 73: 5796-5804.
Höök, F., M. Rodahl, P. Brzezinski, and B. Kasemo. 1998. J.Colloid Interface Sci. 208: 63-67.
Höök, F., J. Vörös, M. Rodahl, R. Kurrat, P. Böni, J. J. Ramsden, M. Textor, N. D. Spencer, P. Tengvall, J. Gold, and B. Kasemo. 2002. Colloids and Surfaces : Biointerfaces 24: 155-170.
Kaur, J., K. V. Singh, A. H. Schmid, G. C. Varshney, C. R. Suri, and M. Raje. 2004. Biosens. Bioelectron. 20: 284-293.
Kim, N., and I.-S. Park. 2003. Biosens. Bioelectron. 18: 1101-1107.
Kösslinger, C., E. Uttenhaler, S. Drost, F. Aberl, F. Wolf, G. Brink, A. Stanglmaier, and E. Sackmann. 1995. Sens. Actuators B 24-25: 107-112.
Laibinis, P. E., C. B. Chain, and G. M. Whitesides. 1991. J. Phys. Chem. 95: 7017.
Laibinis, P. E., R. G. Nuzzo, and G. M. Whitesides. 1992. J. Phys. Chem. 96: 5097-5105.
Lieberg, B., B. Ivarsson, I. Lundstroem, and W. R. Salaneck. 1985. Progress in Colloid & Polymer Sci. 70: 67-75.
Lin, H.-C., and W.-C. Tsai. 2003. Biosens. Bioelectron. 18: 1479-1483.
Liu, Y.-C., C.-M. Wang, and K.-P. Hsiung. 2001. Anal. Biochem. 299: 130-135.
Lord, M. S., M. H. Stenzel, A. Simmona, and B. K. Milthorpe. 2006. Biomaterials 27: 1341-1345.
Lu, B., M. R. Smyth, and R. O'Kennedy. 1996. Analyst 121: 29R-32R.
Lu, H.-C., H.-M. Chen, Y.-S. Lin, and J.-W. Lin. 2000. Biotechnol. Prog. 16: 116-124.
Lucklum, R., and P. Hauptmann. 2000a. Electrochimica Acta 45: 3907-3916.
—. 2000b. Sens. Actuators, B 70: 30-36.
Michalzik, M., J. Wendler, J. Rabe, S. Buttgenbach, and U. Bilitewski. 2005a. Sens. Actuators B 105: 508-515.
Michalzik, M., R. Wilke, and S. Buttgenbach. 2005b. Sens. Actuators B 111-112: 410-415.
Moks, T., L. Abrahmsen, B. Nilsson, U. Hellman, J. Sjoquist, and M. Uhlen. 1986. Eur. J. Biochem. 156: 637-643.
Muramatsu, H., J. M. Dicks, E. Tamiya, and I. Karube. 1987. Anal. Chem. 59.
Nellen, P. M., K. Tiefenthaler, and W. Lukosz. 1988. Sens. Actuators B 15: 285-292.
Nuzzo, R. G., L. H. Dubois, and D. L. Allara. 1990. J. Am. Chem. Soc. 112: 558-569.
Olsen, E. V., S. T. Pathirana, A. M. Samoylov, J. M. Barbaree, B. A. Chin, W. C. Neely, and V. Vodyanoy. 2003. J. Microbiol. Methods 53: 273-285.
Ouerghi, O., A. Touhami, N. Jaffrezic-Renault, C. Martelet, H. Ben Ouada, and S. Cosnier. 2002. Bioelectrochem. 56: 131-133.
Pei, R., Z. Cheng, E. Wang, and X. Yang. 2001. Biosens. Bioelectron. 16: 355-361.
Porter, A. J., T. B. Bright, D. L. Allara, and C. E. D. Chidsey. 1987a. J. Am. Chem. Soc. 109: 3559-3568.
Porter, M. D., T. B. Bright, D. L. Allara, and C. E. D. Chidsey. 1987b. J. Am. Chem. Soc. 109: 3559-3568.
Pradier, C. M., M. Salmain, L. Zheng, and G. Jaouen. 2002. Surface Sci. 502-503: 193-202.
Pribyl, J., M. Hepel, J. Halamek, and P. Skladal. 2003. Sens. Actuators B 91: 333-341.
Quinn, J., P. Patel, B. Fitzpatrick, B. Manning, P. Dillon, S. Daly, R. O'Kennedy, M. Alcocer, H. Lee, M. Morgan, and K. Lang. 1999. Biosens. Bioelectron. 14: 587-595.
Rodahl, M., F. Höök, and B. Kasemo. 1996. Anal. Chem. 68: 2219-2227.

Saha, K., F. Bender, and E. Gizeli. 2003. Anal. Chem. 75: 835-842.
Sakai, G., S. Nakata, T. Uda, N. Miura, and N. Yamazoe. 1999. Electrochim. Acta 44: 3849-3854.
Sauerbrey, G. 1959. Zeitschrift für Physik 155: 206-222.
Shen, Z., G. A. Stryker, R. L. Mernaugh, L. Yu, H. Yan, and X. Zeng. 2005. Anal. Chem. 77: 797-805.
Shons, A., F. Dorman, and J. Najarian. 1972. J. Biomedical Mater. Res. 6: 565-570.
Soh, N., T. Tokuda, T. Watanabe, K. Mishima, T. Imato, T. Masadome, Y. Asano, S. Okutani, O. Niwa, and S. Brown. 2003. Talanta 60: 733-745.
Su, X.-L., F. T. Chew, and S. F. Y. Li. 1999. Anal. Biochem. 273: 66-72.
Su, X.-L., and Y. Li. 2004. Biosens. Bioelectron. 19: 563-574.
—. 2005. Biosens. Bioelectron. 21: 840-848.
Susmel, S., G. G. Guilbault, and C. K. O'Sullivan. 2003. Biosens. Bioelectron. 18: 881-889.
Tang, A. X. J., M. Pravada, G. G. Guilbault, S. Piletsky, and A. P. F. Turner. 2002. Anal. Chim. Acta 471: 33-40.
Voivona, M. V., M. Jonson, and B. Kasemo. 2002. Biosens. Bioelectron. 17: 835-841.
Whitesides, G. M., and P. E. Laibinis. 1990. Langmuir 6: 87-96.
Wink, T., S. J. van Zuilen, B. A, and W. P. van Bennkom. 1997. Analyst 122: 43.
Zhou, J., J. M. Friedt, A. Angelova, K. H. Choi, W. Laureyn, F. Frederix, L. A. Francis, A. Campitelli, Y. Engelborghs, and G. Borghs. 2004. Langmuir: 5878-5878.

Figure captions

Figure 1. Increase of the amide I+II bands area (left axis) and normalized frequency shifts at the 3rd overtone (right axis) in the course of elaboration of the sensors and in the presence of diluted goat serum in PBS (0.15% v/v) and anti-rIgG in PBS (20 mg/L)

a) on the $rIgG_{cov}$ sensing surface, b) on the $rIgG_{PrA}$ sensing surface.

Relative standard deviations were estimated to be equal to 2 Hz on each Δf value and 0.1 a.u. on each IR area.

Figure 2. Frequency response upon successive injections of rIgG, BSA, diluted goat serum and anti-rIgG in diluted goat serum a) of mixed SAM coated quartz crystal (after activation by NHS and EDC) over time, b) PrA-coated quartz crystal.

Figure 3. Dissipation dependence of the normalized frequency shift upon binding of anti-rIgG to $rIgG_{PrA}$ and $rIgG_{cov}$ surfaces.

Figure 4. PM-RAIRS response of the $rIgG_{PrA}$ sensing surface to increasing concentrations of anti-rIgG labelled by cobalt-carbonyl probes in PBS containing goat serum (0.15% v/v)
In the inset: Correlation between the area of the ν_{MCO} bands and the area of the amide I + II bands. Relative standard deviations were estimated to be equal to 0.1 a.u. on each IR area value.

Figure 5. Determination of the affinity constant between anti-rIgG and immobilized rIgG by PM-RAIRS. (a) Experimental data and non linear curve fitting for the $rIgG_{PrA}$ sensing surface. (b) Experimental data and non linear curve fitting for the $rIgG_{cov}$ sensing surface. Relative standard deviations were estimated to be equal to 0.1 u.a. on each IR area value.

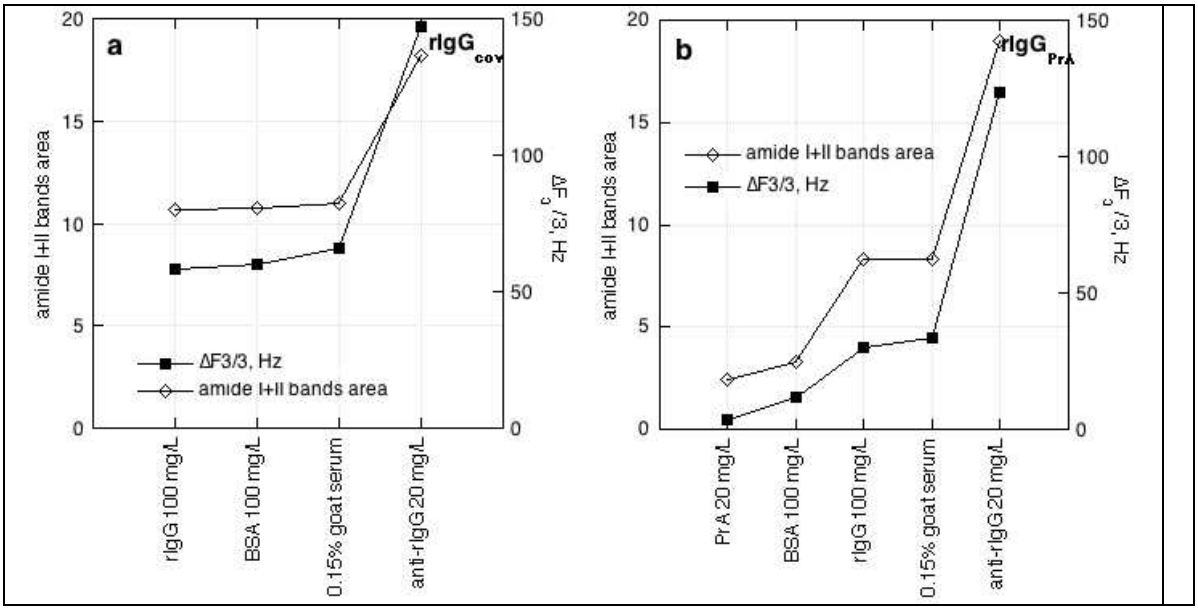

Figure 1

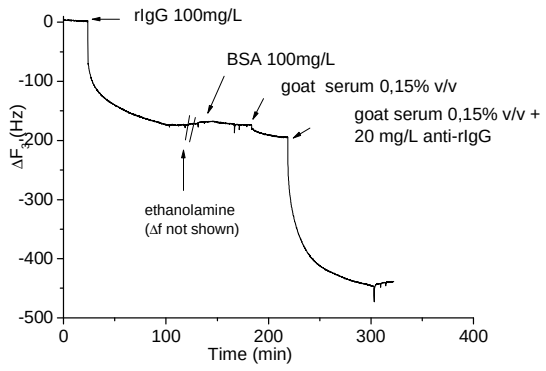

Figure 2a

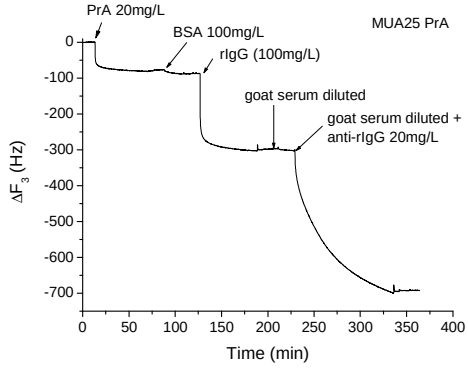

Figure 2b

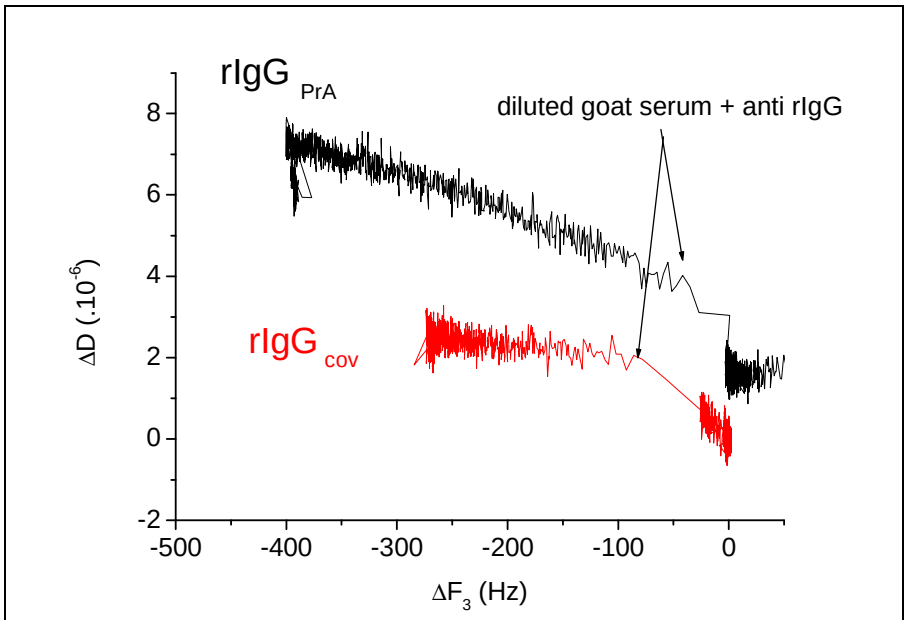

Figure 3

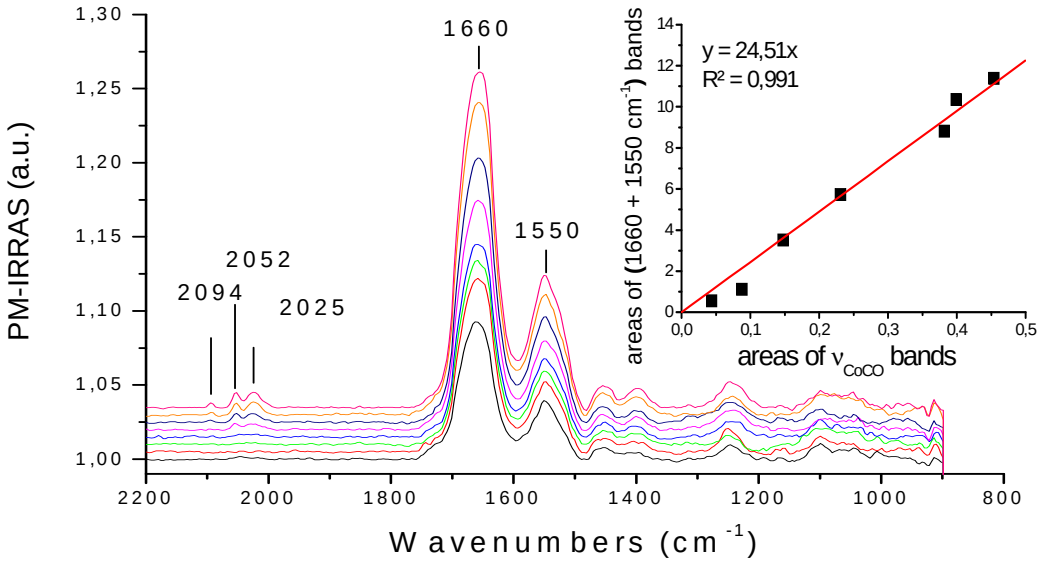

Figure 4

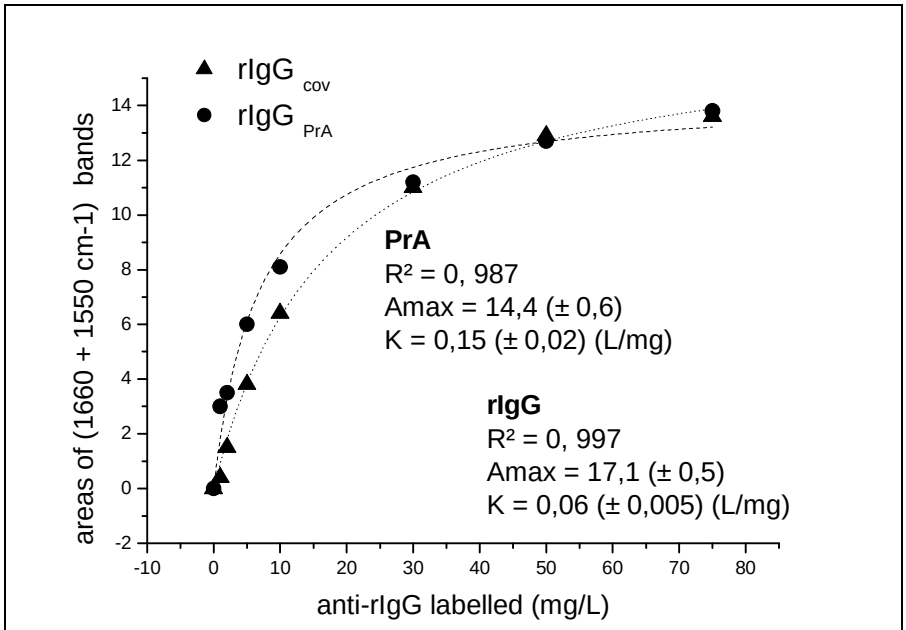
rIgG cov
rIgG PrA
areas of (1660 + 1550 cm-1) bands
anti-rIgG labelled (mg/L)
PrA
R² = 0, 987
Amax = 14,4 (± 0,6)
K = 0,15 (± 0,02) (L/mg)
rIgG
R² = 0, 997
Amax = 17,1 (± 0,5)
K = 0,06 (± 0,005) (L/mg)

Figure 5